Lateral Coupling in Baroclinically Unstable Flows

MICHAEL A. SPALL AND JOSEPH PEDLOSKY

Department of Physical Oceanography, Woods Hole Oceanographic Institution, Woods Hole, Massachusetts

ABSTRACT

A two-layer quasigeostrophic model in a channel is used to study the influence of lateral displacements of regions of different sign mean potential vorticity gradient (Π_y) on the growth rate and structure of linearly unstable waves. The mean state is very idealized, with a region of positive Π_y in the upper layer and a region of negative Π_y in the lower layer; elsewhere Π_y is zero. The growth rate and structure of the model's unstable waves are quite sensitive to the amount of overlap between the two regions. For large amounts of overlap (more than several internal deformation radii), the channel modes described by Phillips' model are recovered. The growth rate decreases abruptly as the amount of overlap decreases below the internal deformation radius. However, unstable modes are also found for cases in which the two nonzero Π_y regions are separated far apart. In these cases, the wavenumber of the unstable waves decreases such that the aspect ratio of the wave remains $O(1)$. The waves are characterized by a large-scale barotropic component that has maximum amplitude near one boundary but extends all the way across the channel to the opposite boundary. Near the boundaries, the wave is of mixed barotropic–baroclinic structure with cross-front scales on the order of the internal deformation radius. The perturbation heat flux is concentrated near the nonzero Π_y regions, but the perturbation momentum flux extends all the way across the channel. The perturbation fluxes act to reduce the isopycnal slopes near the channel boundaries and to transmit zonal momentum from the region of $\Pi_y > 0$ to the region on the opposite side of the channel where $\Pi_y < 0$. These nonzero perturbation momentum fluxes are found even for a mean state that has no lateral shear in the velocity field.

1. Introduction

A necessary condition for the instability of baroclinic flows is that the lateral gradient of the mean potential vorticity must change sign somewhere within the fluid (Charney and Stern 1962; Pedlosky 1964). This result is derived from consideration of global integrals of the momentum budget for a mean flow with an assumed perturbation of wavelike horizontal structure. While this constraint has proved quite useful for identifying flows that are likely susceptible to baroclinic instability, it is not a sufficient condition for instability and does not consider the locations of the regions with differing signs of the potential vorticity gradient.

Our interest in the relative positioning of regions of opposite sign potential vorticity gradient is motivated by an observational and modeling study of a boundary current along the northern slope of Alaska (Spall et al.

2008). The boundary current is composed of low potential vorticity water that is flowing eastward in a bottom-intensified jet over sloping topography (Fig. 1). This structure gives rise to a positive meridional gradient in potential vorticity at the core of the boundary current ($\Pi_y > 0$ near 100-m depth) and a negative gradient in potential vorticity at the base of the boundary current ($\Pi_y < 0$ near 180-m depth). A similar potential vorticity profile is found in an idealized numerical model of this flow. The boundary currents in both the model and the observations are highly time dependent and analysis of the energy conversion terms indicates that the source of the variability is baroclinic instability of the mean flow. Interestingly, the boundary current in the model is found to become more stable as the bottom slope is decreased. This is in opposite sense to what would be expected for a horizontally homogeneous baroclinic flow over a sloping bottom (e.g., Blumsack and Gierasch 1972), where a bottom slope of this sense stabilizes the flow.

For a vertical wall, or very steep bottom slopes, the region of positive Π_y in a baroclinic boundary current

Corresponding author address: Michael Spall, MS#21, 360 Woods Hole Road, Woods Hole, MA 02543.
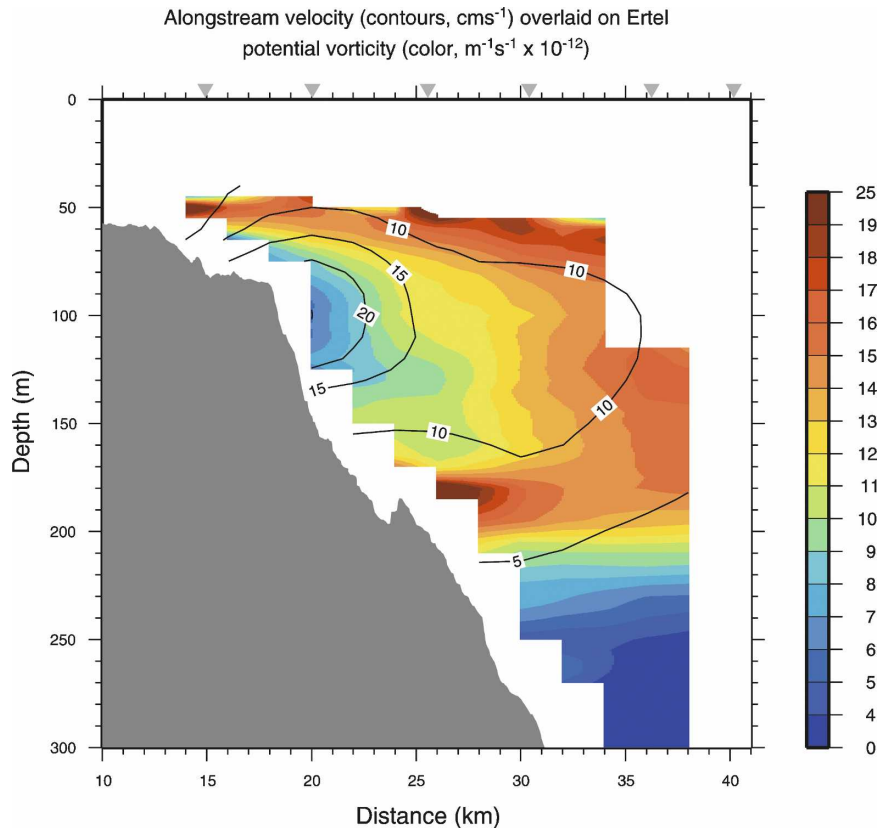E-mail: mspall@whoi.edu

Alongstream velocity (contours, cms^{-1}) overlaid on Ertel
potential vorticity (color, m^{-1}s^{-1} x 10^{-12})

FIG. 1. Mean potential vorticity (colors; m^{-1} s^{-1} × 10^{-12}) overlaid with mean zonal velocity (cm s^{-1}) from a mooring array along the north slope of Alaska, described further in Spall et al. (2008).

will be positioned above the region of negative Π_y. This provides a useful framework for the classical assumption that the lateral gradients of potential vorticity are constant at each depth in the fluid, or within each layer (Charney 1947; Eady 1949; Phillips 1954). However, for sufficiently weak bottom slopes, the upper part of the boundary current can become laterally offset from the lower part of the boundary current. For a boundary current of width equal to the internal deformation radius, this decoupling occurs when the bottom slope is less than f/N, where f is the Coriolis parameter and N is the Brunt–Väisälä frequency. The topographic stabilization found numerically by Spall et al. (2008) occurs near this value of bottom slope, and suggests that the lateral offset of the regions of differing Π_y resulting from the sloping bottom may be the mechanism causing the increased stability.

This example raises the more general issue of how lateral offsets in regions of nonzero mean potential vorticity gradients influence the structure and growth rate of baroclinically unstable waves. One can imagine that such offsets might arise from numerous different flow configurations, the above topographically modified current being just one example. Other examples include boundary currents on opposite sides of a basin or ridge, and outflows from a marginal sea or estuary merging with adjacent currents. Although the model is very idealized, the approach adopted here allows us to isolate the baroclinic waves from barotropic or mixed instabilities and to isolate the effects of the relative positioning of the nonzero Π_y regions.

2. The two-layer QG model

Following Phillips (1954), a two-layer quasigeostrophic (QG) approximation is used to represent the flow. The layer approximation filters out small-scale modes of instability and reduces the partial differential equation to a coupled set of ordinary differential equations. The approach follows the usual linear stability analysis, as can be found in, for example, Pedlosky (1987). The nondimensional equation for the perturbation potential vorticity q_n may be written as

$$\left(\frac{\partial}{\partial t} + U_n \frac{\partial}{\partial x}\right) q_n + \frac{\partial \phi_n}{\partial x} \frac{\partial \Pi_n}{\partial y} = 0, \qquad (1)$$

where U_n is the mean zonal velocity, Π_n is the mean potential vorticity, ϕ_n is the perturbation streamfunction, and $q_n = \nabla^2 \phi_n - F_n(-1)^n(\phi_2 - \phi_1)$ is the perturbation potential vorticity for layer n. The parameter $F_n = (L_0/L_d)^2$, where L_d is the internal deformation radius and L_0 is a horizontal length scale.

Normal-mode solutions for the perturbations are sought, such that

$$\phi_n = \text{Re}\Phi_n(y)e^{ik(x-ct)}. \qquad (2)$$

Substitution of (2) into (1) yields a coupled set of ordinary differential equations:

$$(U_n - c)[\Phi_{nyy} - k^2\Phi_n + (-1)^nF_n(\Phi_1 - \Phi_2)]$$
$$+ \Pi_{ny}\Phi_n = 0, \qquad (3)$$

where the subscript y indicates partial differentiation.

The flow is assumed to be confined to a zonal channel of width L (nondimensionalized by the internal deformation radius) with uniform zonal flow within each layer. The lateral boundary conditions are no normal flow, so that

$$\phi_n = 0, \quad y = 0, \quad L. \qquad (4)$$

In general, the mean potential vorticity gradient is composed of the planetary vorticity gradient, the curvature of the mean flow, and the change in layer thickness. For the deep layer, this change in layer thickness may include the effect of a sloping bottom. The neglect of lateral shear in the mean flow eliminates the curvature term, and also eliminates the horizontal shear as a source of energy for the perturbations, ensuring that any unstable modes are a result of baroclinic instability of the mean flow.

The problem statement is completed by specifying the mean potential vorticity gradient in each layer. The relative contributions of the planetary vorticity gradient, bottom slope, and isopycnal slopes do not need to be specified; it is only the total potential vorticity gradient that enters the equations. To study the effect of lateral displacements of regions of differing signs of Π_y in the simplest context, it is assumed that each layer is composed of a region of nonzero gradient and a region of constant Π, as indicated in Fig. 2.

For simplicity, the upper-layer velocity is taken to be one, the deep velocity is set to zero, and the upper- and lower-layer mean thicknesses are taken to be equal. The horizontal length scale is nondimensionalized by the internal deformation radius, so that $F_1 = F_2 = 1$.
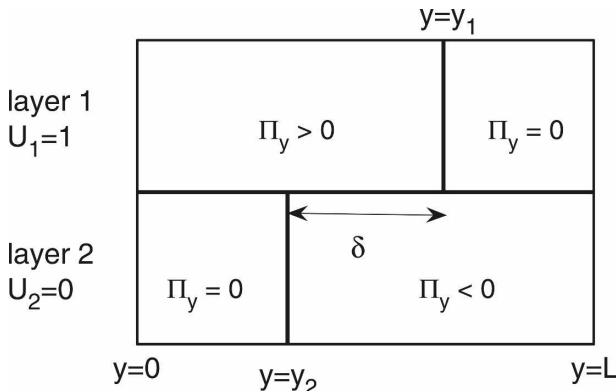

FIG. 2. Two-layer QG model configuration. Regions of nonzero mean potential vorticity gradient overlap by amount δ.

The configuration is completed by specifying the width of the nonzero Π_y region within each layer, indicated by y_1 and $L - y_2$ in Fig. 2. It will be assumed that the nonzero Π gradient regions in each layer are of the same width ($y_1 = L - y_2$) and that the upper-layer region is adjacent to the southern wall and the lower-layer region is adjacent to the northern wall. This is not necessary and, in fact, a number of solutions have been found for general widths of the potential vorticity gradient regions. However, this configuration yields the essential results and reduces the number of parameters that need to be specified.

The matching condition at the interfaces located at y_1 and y_2 is simply that Φ_n and its first derivative are continuous. This is much simpler than the matching condition required for the more general problem where the mean flow strength changes abruptly (e.g., Kamenkovich and Pedlosky 1996).

This configuration is somewhat artificial in that the different regions of mean potential vorticity gradients are implicitly defined by changes in either the bottom slope, the planetary vorticity gradient, or the upper or lower bounding interface slopes. However, the neglect of lateral shear in the mean flow allows us to focus on baroclinic instability as the source of the waves and to isolate the effects of the relative positions of the mean potential vorticity gradient regions from other influences that would arise in a more general problem formulation. Baroclinic conversion is often the dominant source of energy for growing perturbations even in cases that do have significant lateral shear, as found for the observational and modeling study that motivated this work (Spall et al. 2008).

The governing equations form an eigenvalue problem for the complex phase speed c and the eigenfunctions $\Phi_n(y)$. Solutions with a positive imaginary component of the phase speed are sought, indicating expo-
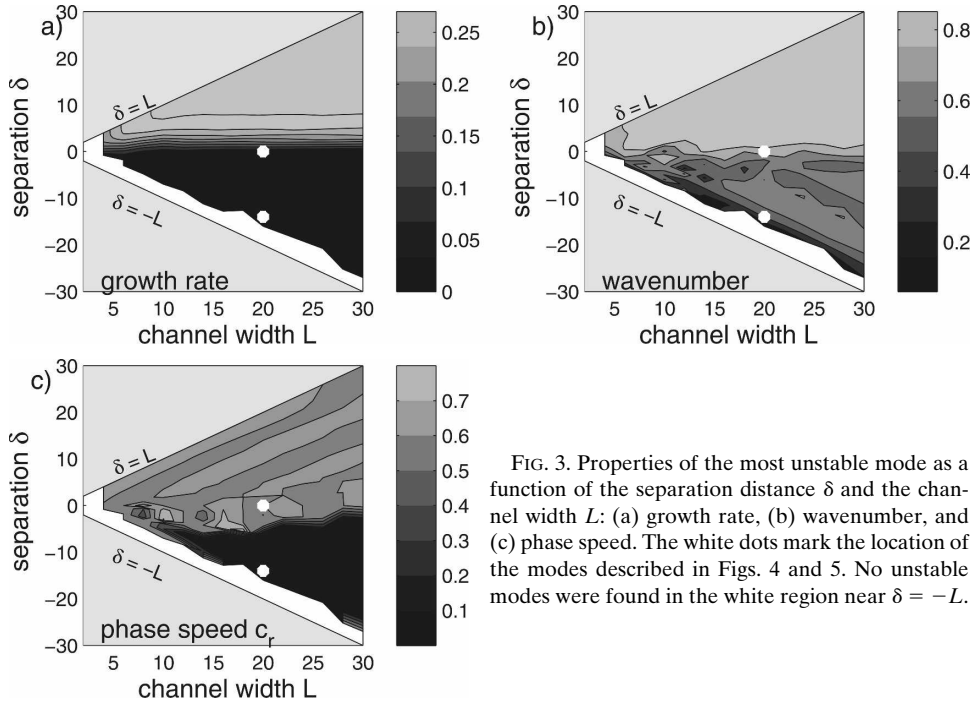
FIG. 3. Properties of the most unstable mode as a function of the separation distance δ and the channel width L: (a) growth rate, (b) wavenumber, and (c) phase speed. The white dots mark the location of the modes described in Figs. 4 and 5. No unstable modes were found in the white region near $\delta = -L$.

nentially growing waves. The governing equations with boundary conditions on Φ are solved using a finite-difference approximation for the continuous Eqs. (3), resulting in a matrix problem for the eigenvalues and eigenfunctions.

3. Results

There are three important horizontal length scales in the problem. The first is the channel width L, the second is the width of the nonzero Π_y regions, and the third is the amount of overlap between these two regions, which for the configurations used here, is $\delta = 2y_1 - L$. If $y_1 = y_2 = L$, so that the nonzero Π_y regions fill the channel, $\delta = L$ and the standard two-layer channel problem of Phillips (1954) is recovered. If $y_1 = L/2$, the two regions each reach to the middle of the channel, but there is no overlap. As $y_1 \to 0$, $\delta \to -L$, and the two regions of nonzero Π_y become isolated near the southern and northern boundaries.

The properties of the most unstable waves are sought as a function of the channel width L and the separation distance δ. The channel width has been varied from 2 to 30 and δ has been varied from $-L$ to L for each channel width. The growth rate of the fastest growing wave is shown in Fig. 3a as a function of the channel width and the separation distance. For very narrow channels, the flow is stable to all perturbations regardless of the separation δ. This limit of stable flow for very narrow chan-

nels is as expected from the standard channel model of Phillips (1954).

Unstable modes emerge as the channel becomes wider and are found for most values of L and δ. The Phillips model result is reproduced along the line $\delta = L$, where the growth rate increases with increasing channel width, most rapidly for narrow channels. Only for very narrow regions of nonzero Π_y is the flow stable ($\delta + L \approx 4$ or $y_1 \approx 2$). Somewhat surprisingly, unstable modes are found even when the nonzero Π_y regions are separated by a very large distance ($\delta \ll 0$). Although the growth rate for $\delta < 0$ is much less than found for the Phillips model in an equivalent width channel, they are the only growing waves supported in this configuration. The growth rate increases abruptly when the two regions begin to overlap ($\delta \gtrsim 0$), but increases only marginally once the two regions overlap by more than a few deformation radii, even for very wide channels.

The wavenumber of the most unstable wave also shows an abrupt transition near $\delta = 0$ (Fig. 3b). For $\delta > 0$, the wavenumber is $O(1)$, as expected for the Phillips model. However, as the two regions become disconnected laterally, the wavenumber decreases. The wavenumber becomes very small as the potential vorticity gradient regions become narrow and far apart, such that the aspect ratio of the growing waves remains $O(1)$.

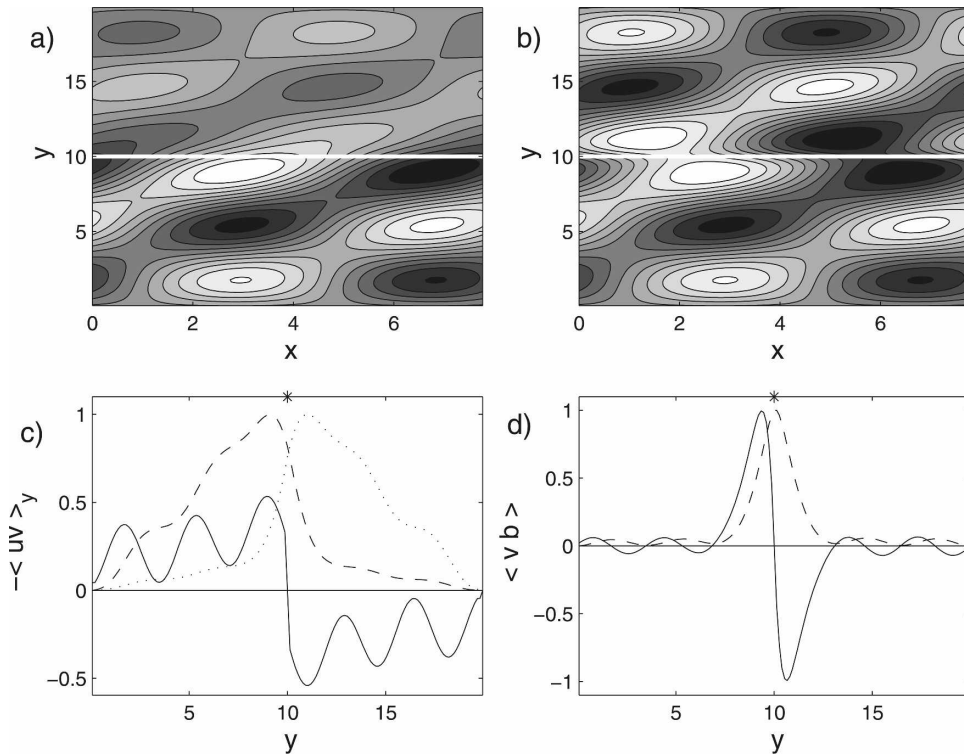The real part of the phase speed is close to 0.5 for $\delta > 0$, again consistent with the Phillips model (Fig. 3c).

FIG. 4. Properties of the most unstable mode for $\delta = 0$ and channel width $L = 20$: (a) upper-layer streamfunction ϕ_1; (b) baroclinic streamfunction ($\phi_1 - \phi_2$); (c) wave momentum flux in layer 1 (dashed line) and layer 2 (dotted line), and total momentum flux divergence (solid line); and (d) wave density flux (dashed line) and wave density flux divergence (solid line). The locations of the upper- and lower-layer nonzero Π_y regions are indicated in (a), (b) by the solid white line and in (c), (d) by the asterisks at the top of the figure.

However, the phase speed is very small for $\delta < 0$. There also exists a set of complementary waves with $\delta < 0$ that have phase speeds close to 1 and equivalent eigenfunctions with y replaced by $L - y$.

There are two dominant types of unstable modes, one for $\delta \geq 0$ and another for $\delta < 0$. Those for $\delta \geq 0$, when the nonzero potential vorticity gradient regions overlap, are analogous to the full channel modes represented by the Phillips model. This is demonstrated by the structure of the most unstable mode for $\delta = 0$, where the two nonzero Π_y regions just touch at the midpoint of the channel. The streamfunction in the upper and lower layers is shown in Fig. 4 for this mode in a channel of width $L = 20$, indicated in Fig. 3 by the uppermost white dot. The eigenfunctions in the two layers are mirror images in y, with the largest amplitudes in the region of nonzero Π_y but also with significant perturbations extending into the zero gradient regions. The waves are composed of both barotropic and baroclinic components. The aspect ratio of the waves $k/l = O(1)$.

The wave momentum flux $\langle uv \rangle$ is shown in Fig. 4c as

a function of latitude for each layer, where $u = -\phi_y$ and $v = \phi_x$ are the perturbation horizontal velocities and $\langle \rangle$ represents the average over a zonal wavelength. The momentum fluxes in each layer are also mirror images of each other and are directed toward the north in both layers. The sum of the eddy flux divergences is given by the solid line. It is everywhere positive in the region where $\Pi_y > 0$ in layer 1 and everywhere negative in the region where $\Pi_y < 0$ in layer 2. This is as expected from the analysis of Held (1975), where it was shown that, in a two-layer QG fluid with an amplifying wave, the total barotropic momentum flux divergence will take the same sign as the weighted sums of the mean potential vorticity gradient provided that the gradient is of the same sign in each layer. In the case of eigenfunctions that are symmetric across the interface between nonzero PV gradients, this makes for a smooth and consistent matching of momentum fluxes with zero flux divergence at the midpoint of the channel. The theory of Held states that the momentum flux divergence must be zero in regions where the mean PV gradient is zero in both layers. The effect of the momentum flux diver-
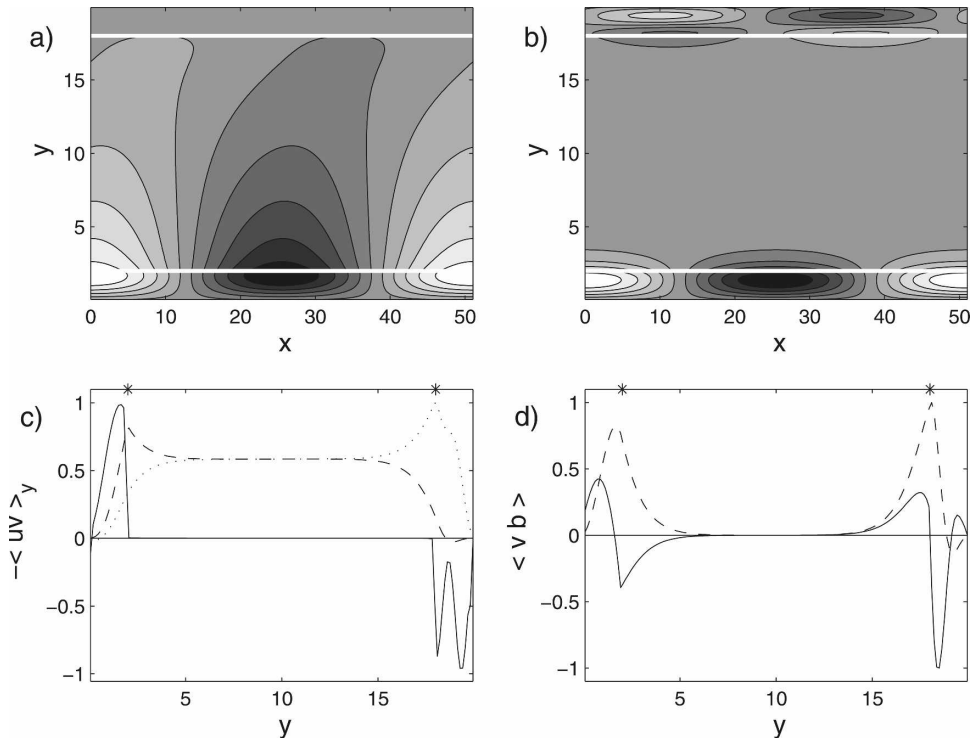
FIG. 5. Properties of the most unstable mode for $\delta = -16$ and channel width $L = 20$, indicated by the lower white dot on Fig. 3: (a) upper-layer streamfunction ψ_1; (b) baroclinic streamfunction $(\phi_1 - \phi_2)$; (c) wave momentum flux in layer 1 (dashed line) and layer 2 (dotted line), and total momentum flux divergence (solid line); and (d) wave density flux (dashed line) and wave density flux divergence (solid line). The locations of the upper- and lower-layer nonzero Π_y regions are indicated in (a), (b) by the solid white lines and in (c), (d) by the asterisks at the top of the figure.

gence is to decelerate the mean flow in the region where $\Pi_y > 0$ and to accelerate the flow in the region where $\Pi_y < 0$.

It is interesting that there exists a nonzero meridional flux, and meridional flux divergence, of zonal momentum even though the mean zonal flow in each layer is uniform. The momentum flux divergence extends well away from the interface where the two potential vorticity gradient regions touch, so that the lateral scale of the eddy momentum flux is set by the channel width and not the internal deformation radius. The eddy potential vorticity flux is downgradient, such that low potential vorticity is fluxed northward. Because it is the potential vorticity flux, and not the momentum flux, that governs the growing waves, this downgradient flux of potential vorticity results in a momentum flux divergence even in a flow that has no lateral gradients in the mean zonal velocity. The result of such growing waves is to introduce mean velocity gradients by extracting zonal momentum from the southern region, where $\Pi_y > 0$, and depositing this momentum in the northern region where $\Pi_y < 0$.

The meridional density flux $\langle v(\phi_1 - \phi_2)\rangle$ is shown in

Fig. 4d as a function of latitude. The flux is everywhere northward, with a peak centered at the midpoint of the channel. The width of the region with significant eddy density flux is on the order of the internal deformation radius. The flux divergence is positive where $\Pi_y > 0$ and negative where $\Pi_y < 0$. This is equivalent to a northward heat flux that will tend to reduce the isopycnal slope within a few internal deformation radii of the center of the channel. As δ is increased, so that the regions of nonzero Π_y begin to overlap, the width of this region of northward heat flux increases, smoothly approaching the half-wavelength sinusoidal profile of the fastest growing wave in the Phillips model as $\delta \to L$.

The second type of unstable mode is found for configurations in which the nonzero Π_y regions do not overlap. The growth rate for these modes is much less than for the previously discussed modes, but they are found consistently over δ and L space, provided that $\delta < 0$ and that the width of the nonzero gradient regions is greater than a few internal deformation radii. A typical wave structure is indicated in Fig. 5. The growing waves are dominated by a large-scale perturbation propagating along one boundary with a smaller merid-

ional-scale perturbation located along the opposite boundary. The zonal wavelength is now much larger than the internal deformation radius; however, the aspect ratio of the dominant wave, k/l, remains $O(1)$. This allows the perturbations to reach from one boundary to the other, thus connecting the two regions of nonzero Π_y. The bridge across the channel is primarily barotropic, as expected for flows on scales much larger than L_d. However, the perturbations supported on the northern and southern sides of the channel are baroclinic (Fig. 5b). This is as expected for a perturbation induced in a region with gradients in potential vorticity that are different in the two layers.

The eddy momentum flux is positive throughout the domain in both layers 1 and 2 (Fig. 5c). The flux divergence is positive in the region of $\Pi_y > 0$ and negative in the region of $\Pi_y < 0$, again consistent with the results of Held (1975). The flux divergence is also zero throughout the region of zero Π_y. If the flow supports growing waves, then the momentum flux must be out of the southern region and into the northern region, and must also be constant between the two regions. This requires a barotropic perturbation that connects the two regions, as is found here. It is curious that the northern and southern regions have a different meridional wave structure and, in fact, we have not been able to find any purely symmetric modes when $\delta < 0$. This result is explained in the following section in terms of interacting Rossby waves.

The eddy density flux is peaked near the transition regions at y_1 and y_2, and drops to zero in the broad region of zero Π_y. The flux divergence tends to decrease the isopycnal slopes near both transition regions and increase the isopycnal slopes adjacent to the regions of large-eddy density fluxes.

4. An interpretation in terms of interacting waves

To gain further insight into the mechanism that allows instability when the zones of opposite-signed potential vorticity (pv) gradients are widely separated, we consider in this section the characteristics of the waves, each of which is produced by a single zone of nonzero and oppositely signed pv gradients, and search for values of k for which the waves share the same phase speed and have a cross-flow structure that effectively "reaches" across a very broad channel separating the two zones. The coalescence of the modes is a common precondition for instability (e.g., the coalescence of the two boundary waves in the Eady problem). A general discussion of the connection between instability and the coalescence of pv neutral waves can be found in several studies (e.g., Heifetz et al. 2004).

Thus we consider two problems. The first is for the wave riding on the potential vorticity gradient $+1$ in the region $0 \leq y \leq y_o$ embedded in a region that extends from 0 to ∞ with a uniform flow in the upper layer $U_1 = 1$. Since our interest is in the case where the channel is broad and the numerical results indicate that the appropriate value of k will be small and of order L^{-1} we will proceed with the analysis under the approximation $k \ll 1$. In the region $0 \leq y \leq y_o$ the solution that satisfies the boundary condition on $y = 0$ is

$$\phi_1 = A(1 - \alpha_1^2) \sinh\alpha_1 y + B(1 + \alpha_2^2) \sin(\alpha_2 y),$$

(5)

$$\phi_2 = A \sinh\alpha_1 y + B \sin\alpha_2 y,$$

where

$$\alpha_1 = \left[\frac{(5 - 8c + 4c^2)^{1/2}}{2(1 - c)} + \frac{(1 - 2c)}{2(1 - c)} \right]^{1/2},$$ (6)

$$\alpha_2 = \left[\frac{(5 - 8c + 4c^2)^{1/2}}{2(1 - c)} - \frac{(1 - 2c)}{2(1 - c)} \right]^{1/2}.$$

In the region $y \geq y_o$, where the pv gradients are zero (for this wave), the solution can most easily be written in terms of the barotropic and baroclinic modes,

$$\phi_b = C_b e^{-k(y - y_0)},$$ (7)

$$\phi_T = C_T e^{-l(y - y_0)},$$

so that in this region,

$$\phi_1 = \phi_b + \phi_T,$$ (8)

$$\phi_2 = \phi_b - \phi_T.$$

When k is small with respect to one, the baroclinic decay scale is the deformation radius, which in our units yields $l = 2^{1/2}$ (i.e., order 1 and independent of k). The decay scale for the barotropic mode is k^{-1} and can be of order L. The eigenvalue problem connecting k and c is obtained by matching the eigenfunctions and their first derivatives at $y = y_o$. Note that although the pv gradient is discontinuous it is always finite so that continuity of the function and its first derivative follows directly from (3). After some algebra, we obtain the relation

$$k = K_L(c, y_0),$$ (9)

where the function K_L is given in the appendix.

The second wave is produced by the pv gradient in the lower layer in the region $L - y_o \leq y \leq L$. In that region the solution may be written as

$$\phi_1 = R \sinh\gamma_1 (y - L) + Q \sin\gamma_2 (y - L),$$ (10)

$$\phi_2 = R(1 - \gamma_1^2) \sinh\gamma_1 (y - L) + Q(1 + \gamma_2^2) \sin\gamma_2 (y - L),$$

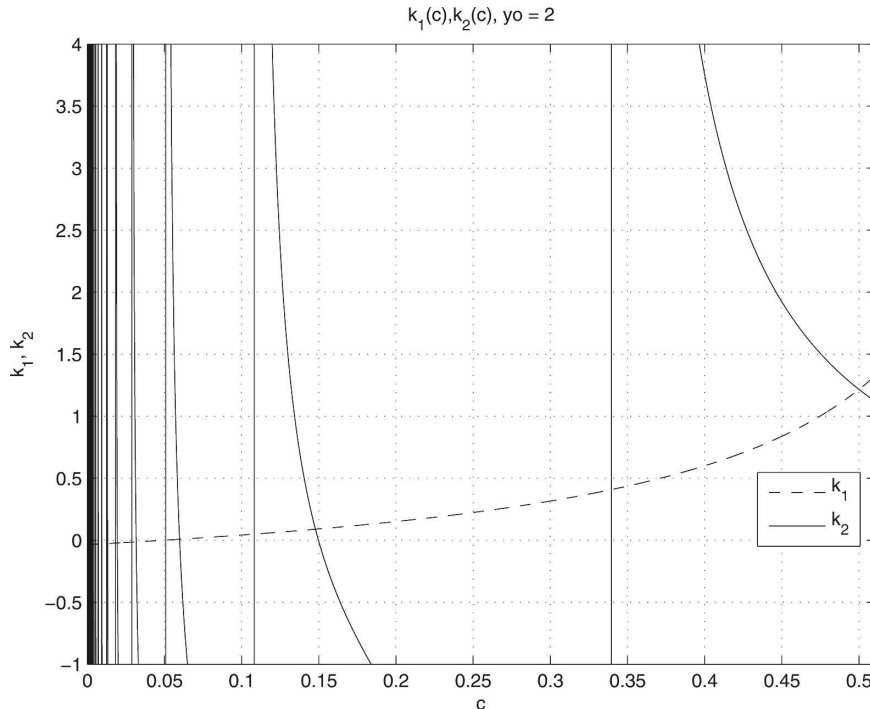FIG. 6. The dispersion relation for $y_0 = 2$, $L = 20$ for the two boundary waves. The intersections are values of potentially unstable modes. Intersections discussed in the text occur at $k = 0.1038$, $c = 0.14748$, and $k = 1.2149$, $c = 0.5$.

where

$$\gamma_1 = \left[\frac{(1 + 4c^2)^{1/2}}{2c} + \frac{2c - 1}{2c} \right]^{1/2}, \quad (11)$$

$$\gamma_2 = \left[\frac{(1 + 4c^2)^{1/2}}{2c} - \frac{2c - 1}{2c} \right]^{1/2}.$$

There is a perfect symmetry between the two waves in which the structure is mirrored. That is clear from Eqs. (5), (6), (10), and (11) in which the waves with c less than 0.5 have rapid variation on the right-hand boundary in the lower layer while waves with phase speeds greater than 0.5 will interchange the structure and have rapid variation in the upper layer as c approaches 1. This will allow us to consider only the interval in c between 0 and 0.5. Larger values of c only reflect the solution around the midpoint of the channel with an interchange of layers. Values of $c = 0.5$ should be symmetric between the two waves and one of the purposes of this calculation is to demonstrate why modes with that speed are not unstable for the broad channel (i.e., when $L \gg y_o$).

The dispersion relation for the wave on the right-hand wall can be written

$$k = K_R(c, y_0). \quad (12)$$

The symmetry of the problem implies, and direct calculation verifies, that K_R has exactly the same form as K_L with $[\alpha_1, \alpha_2] \rightleftharpoons [\gamma_1, \gamma_2]$. Note however that the α's and γ's are different functions of c.

We are interested in those values of k and c that coincide since from those two waves a single mode could be constructed. Figure 6 shows the plot of $k(c)$ for the two waves for the case $y_0 = 2$ and $L = 20$. For this setting of y_o the modes were found numerically to be unstable. The dispersion relation for the left-hand mode is shown as the dashed line. The mode that lives on the pv gradient in the zone near $y = L$ is shown by the solid line. There is clearly an intersection at $c = 0.5$ as there must be by symmetry. However, there are a large number of intersections for small values of c and this is due to the rapid variation of the eigenfunction near the right-hand boundary as noted above; the spatial scale of the variations goes as $c^{1/2}$ so the oscillation becomes increasingly rapid for small c. The identical behavior occurs in the range (0.5, 1) where the rapid variation occurs in the *upper* layer near the *left*-hand wall as c approaches 1.

However, for instability to occur, the two waves generated at the two separate zones must interact and here the quantitative information from the eigenvalue problem is key. The intersection that occurs near $c = 0.5$
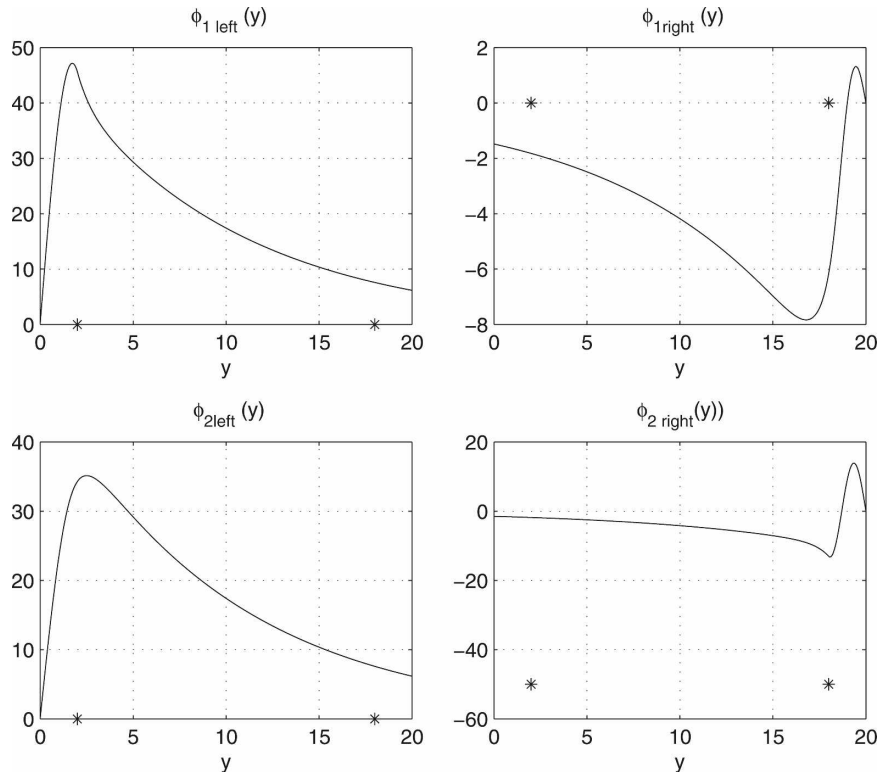
FIG. 7. The eigenfunctions for the two waves sharing the same wavenumber $k = 0.1038$ and $c = 0.1047$. (left) The eigenfunction for the mode on the pv gradient near $y = 0$, for (top) upper and (bottom) lower layer. (right) The wave on the pv gradient near $y = L$. The asterisks show the extent of each of the regions on nonzero pv gradient.

yields an $O(1)$ value of k for each wave. Since the solutions in the region $y_o \le y \le L - y_o$ decay with either k or l, at least one of these must be small so that the modes can reach across the channel to excite and interact with the other region. Now l is always of order one and so it is necessary that k be small. It is the barotropic mode that can provide the bridge between the two regions and produce an instability. Indeed, the baroclinic mode is exponentially small in the intervening region so the excitation of one region by the other is due only to the barotropic mode for large L.

Figure 7 shows the superposition of the two modes for the case of small k (i.e., when the barotropic bridge can link the two regions). On the other hand, for $c = 0.5$, for which the α's and the γ's are equal, k is of order one and the barotropic mode rapidly decays in the interval between the two zones of nonzero pv gradients and so the modes have negligible overlap (Fig. 8). This is consistent with the results of the direct numerical calculation of the unstable modes, which found no unstable modes for $c = 0.5$ unless the two regions of nonzero pv gradient overlapped or were contiguous.

For smaller values of y_o the allowable values of k are

not small and this is also consistent with our inability to find unstable modes for regions of nonzero pv gradients that are too small.

It is interesting to note that the unstable modes are constructed with wave modes that have widely different scales. Within the zone of one of the two regions of nonzero pv gradient the solution always varies rapidly on the scale of the deformation radius in conformance (11) when c is small or (6) for c near unity. This is also consistent with our numerical results that indicate that the widely spaced zones of nonzero pv gradient must themselves be broader than a deformation radius to allow for modes that are locally on that scale.

5. Conclusions

An idealized two-layer quasigeostrophic model has been used to study the influence of lateral displacements of regions of nonzero mean potential vorticity gradient on the structure and growth rate of unstable waves. It has been shown that if the regions in two different layers overlap by as little as the internal deformation radius, modes akin to those produced by the full channel width model of Phillips (1954) are found.
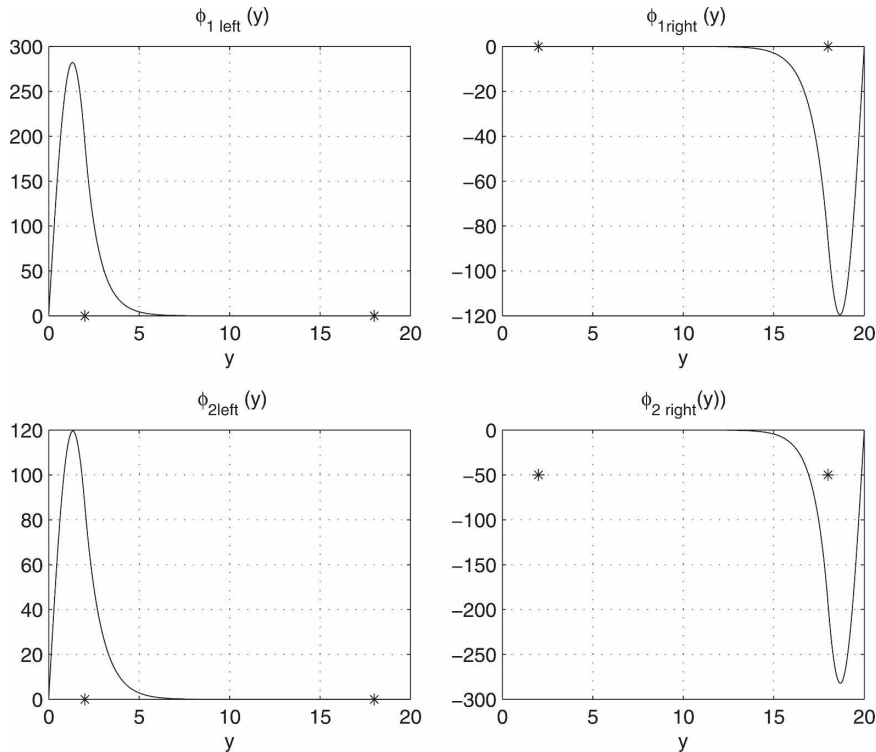
FIG. 8. As in Fig. 7, but for the symmetric mode at $c = 0.5$ that corresponds to $k = 1.2149$. The modes have negligible overlap.

As the nonzero pv gradient regions are separated, the growth rate of the most unstable mode rapidly decreases. However, unstable modes are always found as long as the nonzero pv gradient regions are wider than a couple internal deformation radii, even if the two regions are located on opposite sides of a very wide channel. These waves grow with a time scale of $O(10^{-3} - 10^{-2})L_d/U$, which, for typical ocean parameters, is $O(1\text{year})$. Although these are relatively weak instabilities, they are the only modes present in the system and demonstrate the ability of seemingly distant regions to interact. The perturbations in this case consist of a very long wavelength (on the order of the channel width) barotropic component that is able to span the wide channel. The growing wave is of mixed baroclinic/barotropic structure near the pv gradient regions.

Although very idealized, these results may explain the previous finding that a baroclinic boundary current can be stabilized by a weakening of the bottom slope (Spall et al. 2008) through a lateral shifting of regions of nonzero pv gradient so that they do not overlap.

However, the more surprising and fundamental result of the present study is that the horizontal momentum flux carried by the waves can have a nonzero divergence for a basic flow with no horizontal shear. Nor-

mally one thinks of the lateral shear of the current as being essential for shaping the form of the perturbations to produce a lateral momentum flux. The present calculation emphasizes the important role of the distribution of the potential vorticity gradients, which can accomplish the same result. Such distributions can then induce lateral shear into otherwise uniform currents as a result of upgradient momentum fluxes.

It is also important to note that unstable modes are supported even for cases in which the nonzero pv gradient regions are very far apart. Although their growth rates are relatively small, so that even weak dissipation may render them stable, the development of a barotropic bridge able to connect distant regions of the flow may also have broader applications beyond the specific stability problem explored here.

APPENDIX

The Functions K_L and K_R

The eigenvalue problem is most easily written as a dispersion relation for k as a function of c. For the wave riding on the pv gradient in $0 \leq y \leq y_o$, we obtain

$$K_L = -N_L/D_L, \tag{A1}$$

$$N_L = \cosh\alpha_1 y_0 \cos\alpha_2 y_0 [\alpha_1\alpha_2(\alpha_1^2 + \alpha_2^2)]$$

$$+ \cosh\alpha_1 y_0 \sinh\alpha_2 y_0 \left[\frac{1}{2}\alpha_1\alpha_2^2(2 - \alpha_1^2)\right]$$

$$+ \sinh\alpha_1 y_0 \cos\alpha_2 y_0 \left[\frac{1}{2}\alpha_1^2\alpha_2(2 + \alpha_2^2)\right], \tag{A2}$$

$$D_L = \sinh\alpha_1 y_0 \cos\alpha_2 y_0 \left[\frac{\alpha_2^3}{2}(2 - \alpha_1^2)\right]$$

$$+ \cosh\alpha_1 y_0 \sin\alpha_2 y_0 \left[\frac{\alpha_1^3}{2}(2 + \alpha_2^2)\right]$$

$$\times \sinh\alpha_1 y_0 \sin\alpha_2 y_0 [l(\alpha_1^2 + \alpha_2^2)]. \tag{A3}$$

As explained in the text the function K_R has the same form as K_L with the substitution (α_1, α_2) and $f(\gamma_1, \gamma_2)$.

REFERENCES

Blumsack, S. L., and P. J. Gierasch, 1972: The effects of topography on baroclinic instability. *J. Atmos. Sci.,* **29,** 1081–1089.

Charney, J. G., 1947: The dynamics of long waves in a baroclinic westerly current. *J. Meteor.,* **4,** 135–163.

——, and M. E. Stern, 1962: On the stability of internal baroclinic jets in a rotating atmosphere. *J. Atmos. Sci.,* **19,** 159–172.

Eady, E. T., 1949: Long waves and cyclone waves. *Tellus,* **1,** 33–52.

Heifetz, E., C. H. Bishop, B. J. Hoskins, and J. Methven, 2004: The counter-propagating Rossby-wave perspective on baroclinic instability. I: Mathematical basis. *Quart. J. Roy. Meteor. Soc.,* **130,** 211–231.

Held, I. M., 1975: Momentum transport by quasi-geostrophic eddies. *J. Atmos. Sci.,* **32,** 1494–1497.

Kamenkovich, I. V., and J. Pedlosky, 1996: Radiating instability of nonzonal ocean currents. *J. Phys. Oceanogr.,* **26,** 622–643.

Pedlosky, J., 1964: The stability of currents in the atmosphere and ocean: Part I. *J. Atmos. Sci.,* **21,** 201–219.

——, 1987: *Geophysical Fluid Dynamics.* Springer-Verlag, 710 pp.

Phillips, N. A., 1954: Energy transformations and meridional circulations associated with simple baroclinic waves in a two-level, quasi-geostrophic model. *Tellus,* **6,** 273–286.

Spall, M. A., R. S. Pickart, P. Fratantoni, and A. J. Plueddemann, 2008: Western Arctic shelfbreak eddies: Formation and transport. *J. Phys. Oceanogr.,* in press.